Spatial separation of anaerobic ammonium oxidation and nitrite-dependent anaerobic methane oxidation in permeable riverbeds

Li-dong Shen[1,2], Liao Ouyang[2], Yizhu Zhu[2], Mark Trimmer[2*]

[1]Collaborative Innovation Center on Forecast and Evaluation of Meteorological Disasters, Jiangsu Key Laboratory of Agricultural Meteorology, School of Applied Meteorology, Nanjing University of Information Science and Technology, Nanjing, 210044, China

[2]School of Biological & Chemical Sciences, Queen Mary University of London, London, E1 4NS, UK

[*]E-mail: m.trimmer@qmul.ac.uk

Running title: Spatial separation of anammox and n-damo

This article has been accepted for publication and undergone full peer review but has not been through the copyediting, typesetting, pagination and proofreading process which may lead to differences between this version and the Version of Record. Please cite this article as doi: 10.1111/1462-2920.14554

Originality-Significance Statement

The discovery of anaerobic ammonium oxidation (anammox) and nitrite-dependent anaerobic methane oxidation (n-damo) modified our understanding of both the global nitrogen and carbon cycles. The roles played by anammox and n-damo in these biogeochemical cycles in fresh waters have been increasingly recognized, yet how these two processes compete for their common electron acceptor nitrite, which could govern the fate of fixed nitrogen and methane in fresh waters, is currently unknown. Here, we found a clear spatial separation of anammox and n-damo, with n-damo occupying a narrower range of pore water chemistries in the more reduced, sandy riverbeds compared to that for the more ubiquitous anammox in both gravel and sandy riverbeds. Anammox appears to be favoured in surficial sediment with high NO_2^- concentration, while n-damo prefers deeper sediment with high CH_4 and low O_2 concentrations, suggesting that the pore water NO_2^-, CH_4 and O_2 define distinct spatial distributions for the two processes in permeable riverbed sediments. Furthermore, nitrate reduction by denitrifying bacteria was identified as an important source of nitrite for sustaining both anammox and n-damo. To our knowledge, this is the first study on spatial separation of anammox and n-damo in fresh water sediments.

Summary

Anaerobic ammonium oxidation (anammox) and nitrite-dependent anaerobic methane oxidation (n-damo) play important roles in nitrogen and carbon cycling in fresh waters but we do not know how these two processes compete for their common electron acceptor, nitrite. Here, we investigated the spatial distribution of anammox and n-damo across a range of permeable riverbed sediments. Anammox activity and gene abundance were detected in both gravel and sandy riverbeds and showed a simple, common vertical distribution pattern, while the patterns in n-damo were more complex and n-damo activity was confined to the more reduced, sandy riverbeds. Anammox was most active in surficial sediment (0-2cm), coincident with a peak in *hzs*A gene abundance and nitrite. In contrast, n-damo activity peaked deeper down (4-8cm) in the sandy riverbeds, coincident with a peak in n-damo 16S rRNA gene abundance and higher methane concentration. Pore water nitrite, methane and oxygen were key factors influencing the distribution of these two processes in permeable

riverbeds. Furthermore, both anammox- and n-damo- activity were positively correlated with denitrification activity, suggesting a role for denitrification in supplying both processes with nitrite. Our data reveal spatial separation between anammox and n-damo in permeable riverbed sediments that potentially avoids them competing for nitrite.

Keywords: anammox; n-damo; spatial separation; nitrite; methane; oxygen; permeable riverbeds

Introduction

The process of anaerobic ammonium oxidation (anammox; Equation 1) was discovered in a fluidized-bed reactor (Mulder *et al*., 1995), and later anammox activity was also confirmed in marine sediments in 2002 (Dalsgaard and Thamdrup, 2002). Anammox is mediated by a monophyletic order of bacteria, the Brocadiales (Jetten, 2010). Until now, anammox activity has been reported in various marine systems, including oxygen minimum zones (Kuypers *et al*., 2005; Lam *et al*., 2009; Dalsgaard *et al*., 2012), deep-sea sediments (Byrne *et al*., 2009; Trimmer and Nicholls, 2009; Bale *et al*., 2014) and estuarine sediments (Trimmer *et al*., 2005; Rich *et al*., 2008; Hou *et al*., 2013) and its contribution to N_2 production in marine systems can be higher than 50% (Kuypers *et al*., 2005; Thamdrup *et al*., 2006; Trimmer and Nicholls, 2009). Compared to marine systems, however, far fewer studies have reported anammox activity in rivers (Zhao *et al*., 2013; Zhou *et al*., 2014a; Lansdown *et al*., 2016) and lakes (Schubert *et al*., 2006; Hamersley *et al*., 2009; Wenk *et al*., 2013).

$$NH_4^+ + NO_2^- \rightarrow N_2 + 2H_2O \qquad \Delta G^{0'} = -358 \text{ kJ mol}^{-1}\ NH_4^+ \qquad (1)$$

$$3CH_4 + 8NO_2^- + 8H^+ \rightarrow CO_2 + 4N_2 + 10H_2O \qquad \Delta G^{0'} = -928 \text{ kJ mol}^{-1}\ CH_4 \qquad (2)$$

The process of nitrite-dependent anaerobic methane oxidation (n-damo; Equation 2) was first described in an enrichment culture (Raghoebarsing *et al*., 2006) and is

catalyzed by the bacterium *Candidatus* Methylomirabilis oxyfera (Ettwig *et al*., 2010). Molecular and isotopic evidence for the n-damo bacteria has been recorded in freshwater wetlands (Zhu *et al*., 2012; Hu *et al*., 2014; Shen *et al*., 2017), agricultural soils (Shen *et al*., 2014; Vaksmaa *et al*., 2016; Zhu *et al*., 2018), lake (Deutzmann and Schink, 2011; Deutzmann *et al*., 2014; Graf *et al*., 2018) and estuarine sediments (Shen *et al*., 2016; Wang *et al*., 2018; Zhang *et al*., 2018). Very recently, a high n-damo potential of up to 61.0 nmol CO_2 g^{-1} (dry sediment) d^{-1} was reported in permeable sandy riverbed sediments where it oxidizes approximately 35% of riverbed methane (Shen *et al*., 2018).

As anammox and n-damo are both dependent on nitrite for an electron acceptor, and as the concentration of nitrite is typically low in aquatic ecosystems, anammox and n-damo may compete for nitrite and this ecological interaction could govern the fate of either ammonia (Dalsgaard and Thamdrup, 2002) or methane (Deutzmann *et al*., 2014) in fresh waters. However, until now, little is known about the interaction between anammox and n-damo. A few studies have reported different distributions for anammox and n-damo bacteria in terrestrial soils, with anammox primarily being present in surface soil layers and n-damo deeper down (Shen *et al*., 2014; Hui *et al*., 2017), but which factors control the spatial distribution and magnitude of the two processes is unknown.

Currently our appreciation of rivers as biogeochemical hotspots is being revised. Rivers can remove approximately 40% of nitrogen loading from the terrestrial landscape, acting as important sinks for excess bioavailable nitrogen (Galloway *et al*., 2004). In addition, contemporary analyses suggest that the contribution from running waters (rivers and streams) to the global methane budget is far greater than that estimated only eight years ago (Bastviken *et al*., 2011; Stanley *et al*., 2016). In addition, permeable riverbed sediments allow greater advective flux of inorganic nitrogen and methane through the riverbed than impermeable silts and clays, making them potentially suitable for supporting both anammox and n-damo bacterial communities (Lansdown *et al*., 2016; Shen *et al*., 2018). Hence, permeable riverbed sediments serve as an ideal environment for studying the interaction between anammox and n-damo bacteria.

Here, we asked two questions: 1) do anammox and n-damo actually coexist or are they predominantly spatially separated in permeable riverbed sediments? 2) What factors control the spatial distribution of these two processes? To answer the two questions we investigated the spatial distribution and controls of anammox and n-damo (both activities and gene abundance) in a range permeable riverbeds with natural gradients of nutrients, methane and oxygen and where previously we defined the sandy riverbeds as being more reduced than the gravels (Shen *et al*., 2018). In

addition, we also measured denitrification activity, and *nar*G and *nap*A (encoding the catalytic subunits of the membrane-bound and periplasmic nitrate reductases, respectively) gene abundances in the riverbeds to characterise any potential relationships between denitrification – as a source of nitrite - and anammox and n-damo. In theory, dissimilatory nitrate reduction to ammonium (DNRA) could also supply nitrite for anammox and n-damo; however, our previous work found DNRA activity to be negligible compared to denitrification in similar permeable riverbeds (Lansdown *et al*., 2016; Shelley *et al*., 2017). Therefore, the DNRA activity and its responsible functional genes were not examined in this study.

Results

Physiochemical characteristics

Sediment and pore water were collected from seven permeable riverbeds, including three gravel riverbeds (River Stour I, River Stour II and River Lambourn) and four sandy riverbeds (Hammer Stream, River Medway, River Marden and River Nadder) with average grain sizes of typically 2-10 mm and 0.28-2 mm, respectively (Shelley *et al*., 2014, 2017; Lansdown *et al*., 2016) in southeast England (Fig. S1). The physicochemical characteristics of the riverbed pore water are shown in Fig. S2.

Principle component analysis (PCA) was used to compare the pore water chemistries of the different riverbeds (Fig. 1A), where a sharp separation of O_2 and CH_4, along PC1 (accounted for 51% of the variance), suggested an axis from less reduced to more reduced pore waters (see Shen *et al*., 2018 for further details). All of the riverbed sediments could be classified into three groups according to their fine-scale pore water chemistries: the Hammer Stream, with low O_2 and high CH_4 concentrations (red circles in Fig. 1A); the remaining sandy riverbeds, with intermediate O_2 and CH_4 concentrations (blue circles); and the gravel riverbeds with high O_2 and low CH_4 concentrations (magenta circles).

Potential rates of both anammox and n-damo

No significant accumulation of either $^{29}N_2$ or $^{30}N_2$ was measured in any anoxic slurries amended with $^{15}NH_4^+$ only (Table S1), confirming that any residual pore water oxygen or NO_x^- had been consumed during the pre-incubation period. When $^{15}NH_4^+$ and $^{14}NO_3^-$ were added together, $^{29}N_2$ accumulated linearly with incubation time in every slurry and without any accumulation of $^{30}N_2$ (Table S1), confirming the presence of potential anammox activity. We also measured significant accumulation of both $^{29}N_2$ and $^{30}N_2$ in all of the slurries amended with $^{15}NO_3^-$ only (Table S1), confirming the co-occurrence of anammox and denitrification activity. An anammox potential was found in all gravel and sandy riverbed sediments (Fig. 1B), with a

similar range of potential anammox activity, from 1.0 to 38.7 nmol N_2 g^{-1} (dry sediment) d^{-1}, in both sediment types (Table S2).

The vertical distribution of anammox activity was very similar across all riverbeds, being characterised by a single smoother term (Generalised Additive Mixed-Effects Model, GAMMs; Fig. 2A). Anammox activity peaked consistently in the upper 2cm layer of sediment and then decreased with depth (Fig. 2A). The greatest depth-specific values for the relative contribution (*ra*%) from anammox to sediment N_2 production were recorded in the upper 4cm of sediment (Fig. S3). The *ra*% values were 5.9%, 9.4%, 12.3%, 5.7%, 5.4%, 6.0% and 4.7%, on average, in the Hammer Stream and rivers Medway, Marden, Nadder, Stour I, Stour II and Lambourn, respectively.

Our recent study on anaerobic methane oxidation (Shen *et al*., 2018) in these riverbed sediments, showed that the addition of both NO_2^- and NO_3^-, in combination with $^{13}CH_4$, resulted in $^{13}CO_2$ production in the more reduced, sandy riverbeds (Fig. 1C), but not with sediments from the more oxic, gravel riverbeds and here we focus on just n-damo driven by NO_2^-. The potential for n-damo measured in slurries amended with $^{13}CH_4$ and NO_2^- in the Hammer Stream (12.2-61.0 nmol CO_2 g^{-1} (dry sediment) d^{-1}), was significantly greater (p<0.05) than that measured in the rivers Medway (1.4-10.9 nmol CO_2 g^{-1} (dry sediment) d^{-1}), Marden (1.2-7.0 nmol CO_2 g^{-1}

(dry sediment) d^{-1}) and Nadder (0.4-1.1 nmol CO_2 g^{-1} (dry sediment) d^{-1}) (Table S2).

In comparison to anammox, the depth distribution patterns for n-damo were more complex, with multiple GAMMs (*see* Experimental procedures) being required to characterise the patterns in the data (p>0.05, Fig. 2C). Similarly, we divided the data into the three different groups as described above: the Hammer Stream, with high n-damo potential; the remaining sandy riverbeds, with intermediate n-damo potential; and the gravel riverbeds, with no measurable n-damo potential (Fig. 2C). Potential n-damo activity peaked below anammox, at 2-4cm into the bed in the rivers Medway, Marden and Nadder, and, at 4-8cm, in the Hammer Stream (Fig. 2C).

Microbial abundance for anammox and n-damo

Copy numbers of the anammox bacterial *hzs*A (α subunit of the hydrazine synthase) genes varied from 5.6×10^4 to 6.4×10^5 copies g^{-1} dry sediment, across the seven riverbeds (Table S2). Across the seven riverbeds the abundance of the *hzs*A gene peaked in the upper 2cm layer of the sediment and decreased with depth, in a pattern consistent with anammox activity (Fig. 2B) and, again, could be characterised by a single GAMM smoother.

In contrast to anammox, there was a clear difference in abundance for the n-damo bacterial 16S rRNA genes between the riverbeds (Table S2), as for n-damo

activity. Highest gene abundance was measured in the most reduced sediment of the Hammer Stream (3.7×10^6-1.5×10^7 copies g^{-1} dry sediment), whereas its abundance was an order of magnitude lower in the remaining sandy riverbeds (9.3×10^5-7.5×10^6 copies g^{-1} dry sediment). Although the gravel sediments recorded no significant n-damo potential, they harboured a very low, but measurable, gene abundance of less than 8.7×10^3 copies g^{-1} dry sediment (Shen *et al*., 2018). Similar to the vertical distribution of potential n-damo activity, n-damo bacterial 16S rRNA gene abundance needed multiple GAMM smoothers (*see* Experimental procedures) and could be grouped into: the Hammer Stream, with high n-damo bacterial abundance; the remaining sandy riverbeds, with moderate abundance; and the gravel riverbeds with very low abundance (Fig. 2D). The 16S rRNA gene abundance of n-damo bacteria also peaked below anammox, at 4-8cm into the bed (Fig. 2D).

In addition to n-damo bacteria, the 16S rRNA gene abundance of ANME-2d archaea, catalyzing nitrate-dependent anaerobic methane oxidation (Haroon *et al*., 2013), was also quantified. The ANME-2d archaeal 16S rRNA gene abundance was 2.1×10^4-2.5×10^5 copies g^{-1} dry sediment in the sandy riverbeds, while the gene abundance in the gravel was, again, very low at less than 2.5×10^3 copies g^{-1} dry sediment. The gene abundances of *nap*A and *nar*G genes, encoding the nitrate reductases, were quantified to examine their potential relationship with anammox and

n-damo. The *nap*A gene was far more abundant in the gravel riverbeds (2.1×10^4-9.7×10^5 copies g^{-1} dry sediment) compared to the sands (1.2×10^3-2.6×10^4 copies g^{-1} dry sediment), while, in contrast, the sandy riverbeds contained far higher *nar*G gene abundance (4.0×10^4-8.9×10^5 copies g^{-1} dry sediment) than in the gravels (3.1×10^3-8.8×10^4 copies g^{-1} dry sediment) (Fig. 3).

From the qPCR data, the ratios of anammox bacterial *hzs*A gene abundance, and n-damo bacterial 16S rRNA gene abundance, to total bacterial 16S rRNA gene abundance, were 0.01-0.3% and 0.0008-2.8%, respectively, across all riverbeds. The ratio of ANME-2d archaeal 16S rRNA gene abundance, to total archaeal 16S rRNA gene abundance was 0.01-1.6% across all riverbeds.

Factors controlling the distribution and activity of anammox and n-damo bacteria

The redundancy analysis (RDA) showed that both the anammox and n-damo potentials correlated well with their respective gene abundances: anammox bacterial *hzs*A and n-damo bacterial 16S rRNA, respectively (r =0.407 and 0.815, respectively) (Fig. 4). Most importantly, the RDA showed that anammox separated well from n-damo (Fig. 4), where both anammox activity and anammox bacterial *hzs*A gene abundance were most strongly associated with pore water NO_2^- concentration (r = 0.384 and 0.638, respectively) and n-damo activity and n-damo bacterial 16S rRNA gene abundance were most strongly associated with pore water CH_4 concentration (r

= 0.587 and 0.453, respectively).

Potential denitrification activity was significantly correlated with *nap*A gene abundance (r = 0.657), as well as potential anammox activity (r = 0.510) in all riverbeds (Fig. 5a). We also found a good (non-linear) correlation between potential denitrification activity and n-damo activity in the sandy riverbeds (r = 0.851, Fig. 5b), with n-damo activity increasing steeply at the peak in denitrification activity. In addition, *nar*G gene abundance was significantly correlated with both the n-damo bacterial abundance (r = 0.764) (Fig. 5c) and potential n-damo activity (r = 0.746) (Fig. 5d).

Discussion

Stable isotope experiments and molecular analyses demonstrated presence and activity of anammox bacteria in all permeable riverbeds while presence and activity of n-damo bacteria in only the more reduced, sandy riverbeds, suggesting a broader distribution of anammox bacteria compared to n-damo bacteria. The results also indicated that while anammox represents a sink for fixed nitrogen across permeable riverbeds (Lansdown *et al*., 2016), n-damo only represents a sink for methane under more reduced conditions. Anammox activity in the permeable sandy and gravel

riverbeds can be attributed to a seemingly tight coupling between nitrification and anammox within aggregates (Lansdown *et al*., 2016), with nitrification providing both NO_2^- and anoxic microsites for anammox. The potential interaction between nitrification and anammox has also been indicated in oxygen-limited marine systems (Lam *et al*., 2007, 2009; Yan *et al*., 2010). Although we could detect a low 16S rRNA gene abundance for n-damo bacteria in the gravel riverbeds, we could not measure any actual n-damo activity (Fig. 1C). *Candidatus* Methylomirabilis oxyfera, which oxidizes methane using internally produced oxygen (Ettwig *et al*., 2010; Wu *et al*., 2011), is known to be sensitive to external free oxygen (Luesken *et al*., 2012); though trace oxygen (0.7-1.1% of O_2) has actually been reported to stimulate n-damo activity in enrichment cultures, albeit only moderately (Kampman *et al*., 2018). Sandy riverbeds are recognised as being less permeable than gravels (Lansdown *et al*., 2016; Shen *et al*., 2018) and gravel-beds can contain relatively high oxygen concentrations that likely inhibit both the activity and growth of n-damo bacteria. Even though the bulk pore water of sandy riverbeds still has appreciable oxygen (> 38μM), n-damo can occur in such riverbeds, probably due to the presence of anoxic microsites within aggregates as observed for anammox (Lansdown *et al*., 2016). Further, in the more permeable gravels, it is also likely that the growth and activity of n-damo bacteria are limited by strong competition for methane from aerobic methanotrophs, whose

activity has been recorded in a wide range of gravel riverbeds (Shelley *et al*., 2014, 2015; Trimmer *et al*., 2015). Thus, a higher delivery of oxygen, coupled to far lower methane in the more permeable gravels appears unsuitable for an active n-damo bacterial community and, in the gravels, methane is oxidised aerobically.

The coincident peaks in anammox activity and *hzs*A gene abundance point to the surficial sediment as the preferred habitat for anammox bacteria, which is consistent with previous findings in lake (Zhu *et al*., 2013) and estuarine sediments (Rooks *et al*., 2012; Wang *et al*., 2012). Both anammox activity and gene abundance were positively correlated with pore water NO_2^- concentration (Fig. 4), suggesting that anammox was controlled by NO_2^- availability. Previous studies also suggested that NO_2^- is a key factor for anammox activity in estuarine (Meyer *et al*., 2005) and riverbed sediments (Lansdown *et al*., 2016). Here, we identified no association between pore water NH_4^+ concentration and anammox activity or *hzs*A gene abundance (Fig. 4), as there was relatively more NH_4^+ compared to NO_2^- in the riverbeds (Fig. S2).

Here, neither the maximum in n-damo activity nor its 16S rRNA gene abundance were associated with the NO_2^- peak, with both its activity and abundance occurring deeper down (2-4 and 4-8cm) into the bed, suggesting that n-damo “avoided” competition for nitrite with anammox in the surficial sediment layers. Both n-damo activity and n-damo bacterial 16S rRNA gene abundance were negatively correlated

with pore water oxygen concentration but positively correlated with methane concentration (Fig. 4), indicating that n-damo appears to be favoured in riverbed sediments with higher methane and lower oxygen concentrations, particularly in the Hammer Stream, as for lake sediments (Deutzmann *et al*., 2014), wetland (Hu *et al*., 2014) and paddy soils (Shen *et al*., 2014). The deeper layers of sandy riverbeds had relatively lower oxygen and higher methane concentrations compared with the surficial sediments, which could help to maintain a larger population of n-damo bacteria and higher n-damo activity. The activity of n-damo bacteria was reported to increase significantly with increased methane concentration in a bioreactor (Cai *et al*., 2018). Although other anaerobic methanotrophs may compete with n-damo bacteria for methane, the n-damo process is energetically more favorable per mol of methane oxidised than for nitrate-, sulfate-, and iron-dependent anaerobic methane oxidation (He *et al*., 2018).

Our previous studies have found that denitrification was responsible for the majority (greater than 90%) of in situ nitrate reduction in such permeable riverbed sediments, with DNRA being negligible (Lansdown *et al*., 2016; Shelley *et al*., 2017). Here, both anammox (including the data from all riverbeds; Fig. 5a) and n-damo activity (only the data from the sandy riverbeds where n-damo activity was detected; Fig. 5b) were positively correlated with denitrification activity. This suggests that the

release of NO_2^- from NO_3^- reduction by denitrification might provide an important supply of nitrite for sustaining both anammox and n-damo. Zhou and colleagues (2014b) provided direct evidence for denitrification-dependent anammox activity in riverbed sediments. Hence, anammox appears to couple to either nitrification or denitrification, which may help broaden its distribution across contrasting riverbed sediments. Nitrification could be the major source of NO_2^- for anammox under oxic conditions, as discussed above, while the NO_2^- required for anammox under more reduced conditions may come mainly from denitrification.

Currently it is unknown if the NO_2^- required for n-damo also comes from denitrification and, if so, what is the relative importance of this source. Here, we present the first evidence for a potential interaction between n-damo and denitrification in riverbed sediments. Interestingly, we found that n-damo activity increased exponentially (not linearly as for anammox) with denitrification activity (Fig. 5b). In addition, nitrate-dependent anaerobic methane oxidation, which oxidizes methane through the reduction of NO_3^- to NO_2^-, via a reverse methanogenesis pathway (Haroon *et al*., 2013), could also theoretically provide NO_2^- for n-damo. Our recent study confirmed the co-occurrence of nitrate-dependent anaerobic methane oxidation in these sandy riverbeds (Shen *et al*., 2018), but its activity was an order of magnitude lower than the denitrification activity measured in the current study. Therefore,

denitrification is likely to be the dominant source of NO_2^- for n-damo in our riverbeds. Further, the gene abundance of *nar*G, whose expression is known to predominate under anoxic conditions (Lopez-Gutierrez *et al*., 2004), was positively correlated with n-damo activity and n-damo bacterial 16S rRNA gene abundance (Fig. 5c and 5d), highlighting a potential link between anaerobic nitrate reduction and n-damo, through NO_2^-, in the sandy riverbeds.

In summary, our results show clear spatial separation between anammox and n-damo, with n-damo having a narrower distribution deeper into the more reduced, sandy riverbeds. Anammox appears to be favoured in surficial sediment with high NO_2^- concentration, while n-damo prefers deeper sediment with high CH_4 and low O_2 concentrations, suggesting that the pore water NO_2^-, CH_4 and O_2 define distinct spatial distributions for the two processes in permeable riverbed sediments.

Experimental procedures

Study sites and sample collection

Sediment and pore water were collected from two contrasing types of permeable riverbeds (*n*=7) in southeast England (Fig. S1): less reduced, gravel riverbeds (rivers Lambourn, Stour I and Stour II) and more reduced, sandy riverbeds (Hammer Stream

and rivers Medway, Marden, and Nadder) on seven occasions between February, 2016, and January, 2017, as described previously (Shen *et al*., 2018).

Physiochemical analyses

The surface water and pore water pH and dissolved oxygen (O_2) were measured by pH and O_2 probes, respectively, as described previously (Lansdown *et al*., 2014). The concentrations of dissolved CH_4 in both surface water and pore water were measured by gas chromatography (GC/FID) fitted with a flame ionization detector (Agilent Technologies) according to Shelley and colleagures (2015). The concentrations of surface water and pore water NO_3^-, NO_2^- and NH_4^+ were measured using an auto analyzer (Skalar San^{+2}, Breda, The Netherlands) and standard colorimetry. All the physicochemical parameters were determined in five replicates.

Isotope tracer experiments

Potential rates of anammox and denitrification were determined using ^{15}N isotope pairing methods (Thamdrup and Dalsgaard, 2002). The NO_3^- concentration was up to 580μM in the surface water of the rivers that would require a long pre-incubation to remove it before ^{15}N-NO_3^- could be added. Therefore, ^{14}N-NO_3^- free synthetic river water (Lansdown *et al*., 2016; Shen *et al*., 2018) was used instead of river site-water to make the sediment slurries. Approximately 1g of fresh sediment was transferred

into a 3ml pre-weighed gastight vial (Labco, Lampeter, U.K.), together with 0.9 ml of N_2-degassed synthetic river water. All slurries were prepared inside an anoxic glove box (Belle Technology, UK). To consume any residual oxygen and NO_x^- (NO_3^- and NO_2^-), all of the prepared slurries were preincubated overnight on orbital shakers and the vials then injected with 100μl of N_2-degassed 2mM stock solutions: 1) $^{15}NH_4Cl$ (^{15}N at 98%), 2) $^{15}NH_4Cl$ plus $Na^{14}NO_3^-$ and 3) $Na^{15}NO_3^-$ (^{15}N at 98%) to a final concentration of 200μM and additional slurries were left unamended as controls. The vials were then placed on orbital shakers for a further 6h and then at 0h, 1h, 2h, 3h and 6h, triplicate vials were sacrificed by injecting 100μl of 50% (w/v) $ZnCl_2$ solution. The concentrations of $^{28}N_2$, $^{29}N_2$ and $^{30}N_2$ in the headspace of each vial were measured directly using continuous flow isotope ratio mass spectrometry (CF/IRMS), calibrated with N_2 in He over air-equilibrated water (Delta Plus, Thermo Finnigan) (Trimmer and Nicholls, 2009). The potential rates of anammox and its contribution to sediment N_2 production (*ra*%) were calculated using equations provided previously (Thamdrup and Dalsgaard, 2002; Risgaard-Petersen *et al*., 2004).

Potential rates of n-damo were measured using $^{13}CH_4$ tracing methods according to Shen and colleagues (2018). Briefly, 2-3g of fresh sediment were transferred into 12ml pre-weighed gastight vials (Labco, Lampeter, U.K.), together with 5ml of N_2-degassed synthetic river water (as above), all inside the anoxic glove box. To

remove any background NO_2^- and NO_3^-, the prepared slurries were placed on orbital shakers for both short (6h) and long (2d) pre-incubation times and n-damo activity was confirmed without a lag-phase in slurries with a short pre-incubation time (Shen *et al*., 2018). All the vials were then injected with 100µl of N_2-degassed individual stock solutions containing electron acceptors of NO_2^- ($NaNO_2$, 1mM) or NO_3^- ($NaNO_3$, 2.5 mM). Subsequently, each vial was injected with 50µl of $^{13}CH_4$ using a gastight syringe, to generate a headspace of approximately 1% (v/v) methane and parallel slurries were left unamended as controls. Six replicate vials were sacrificed by injecting 300µl of 50% (w/v) $ZnCl_2$ solution at different intervals. The headspace $^{12}CO_2$ and $^{13}CO_2$ concentrations were also measured using CF/IRMS. Furthermore, after each headspace analysis, the concentration of dissolved inorganic carbon (CO_2 + HCO_3^- + CO_3^{2-}) in each vial was determined as described previously (Trimmer *et al*., 2015). The $^{13}CO_2$ measured from headspace plus ^{13}C-DIC from overlying water equalled the total production of labelled inorganic carbon from ^{13}C-CH_4.

DNA extraction

Genomic DNA was extracted from the sediment using a Power Soil DNA kit (MO BIO Laboratories, Carlsbad, CA, USA) according to the manufacturer's instructions and its concentration and quality determined with a NanoDrop spectrophotometer (ND-1000; Isogen Life Science, the Netherlands).

Quantitative PCR (qPCR)

The primer set hzsA_1597f-hzsA_1857r (Harhangi *et al*., 2012) was used to measure the anammox bacterial *hzs*A gene abundance. The primer set of qp1f-qp1r (Ettwig *et al*., 2009) was used for quantification of the 16S rRNA gene abundance of n-damo bacteria. The 16S rRNA gene abundance of ANME-2d, the archaea catalyzing nitrate-dependent anaerobic methane oxidation (Haroon *et al*., 2013), was determined using the primer set 641F-834R (Schubert *et al*., 2011). The genes encoding the membrane-bound nitrate reductase (Nar) and periplasmic nitrate reductase (Nap) were quantified by the primer sets 1960m2f-2050m2r (Lopez-Gutierrez *et al*., 2004) and *napA* V17F-*napA* 4R (Bru *et al*., 2007), respectively. In addition, the total bacterial and total archaeal 16S rRNA gene abundance was also quantified using the primer sets 341f-518r (Muyzer *et al*., 1993) and Arch967f-Arch1060r (Cadillo-Quiroz *et al*., 2006), respectively, with coverage of most bacteria and archaea. The qPCR thermal program was as follows: 98°C for 3 minutes; 40 cycles of 95°C for 10s, annealing for 25s, and 72°C for 45s; and a final extension at 72°C for 7 minutes. The standard curve was performed with 10^1- to 10^7-fold serial dilutions of plasmid DNA containing the target gene. Three replicates for each sample and three negative controls without template were applied for each qPCR assay. After qPCR, the melting curve analysis was evaluated to further verify the specificity of amplification. The sequences and

target genes of the qPCR primers used can be found in Table S3.

Statistical analyses

Generalized additive mixed effects models (GAMMs) were used to characterise the vertical distribution of both the activities and gene abundances for anammox and n-damo in the riverbeds in R (version 3.1.1) (Table S4). We treated each river as a random effect on the intercept to account for their random deviation from the fixed effects. We firstly fitted rate or gene abundance for n-damo as a function of depth into a full model using the "gamm4" function from the gamm4 package (version 0.2-5). The full model included the groups (i.e., the Hammer Stream; the remaining sandy riverbeds; and the gravel riverbeds) on the intercept, which characterised the median value of the rate or gene abundance of n-damo. To characterise the patterns of depth distribution for n-damo, the full model allowed the shape of depth distribution (cubic regression splines) to vary among the groups. The differences among groups were tested for by comparing the full model with a series of reduced models. For multi-model selection, we calculated small sample-size corrected AICc (Akaike Information Criterion) and AICc weights using the "MuMIn" package (version 1.15.6) and repeated these steps for the gene abundance and activity of anammox bacteria.

Any relationships between pore water chemistry and anammox and n-damo were examined using multivariate techniques (CANOCO, version 4.5) (ter Braak and

Šmilauer, 2002). Principal components analysis (PCA) was first used to characterise any differences in pore water chemistry between rivers and then redundancy analysis (RDA) was used to characterise any potential correlations between anammox and n-damo and gene abundance and those pore water chemistries, with $p<0.05$ as the criterion for significance.

Acknowledgements

This study was supported by the Natural Science Foundation of China (No. 41501261), the China Scholarship Council (CSC), the Natural Science Foundation of Jiangsu Province (No. BK20150893) and Queen Mary University of London. We acknowledge the land owners for allowing us access to the rivers and also thank Ian Sanders, Felicity Shelley and Paul Fletcher for technical and field work assistance.

Conflict of interest

The authors declare no conflict of interest.

References

Bale, N., Villanueva, L., Fan, H., Stal, L.J., Hopmans, E.C., Schouten, S., and

Sinninghe Damsté J.S. (2014) Occurrence and activity of anammox bacteria in surface sediments of the southern North Sea. *FEMS Microbiol Ecol* **89**: 99-110.

Bastviken, D., Tranvik, L.J., Downing, J.A., Crill, P.M., and Enrich-Prast, A. (2011) Freshwater Methane Emissions Offset the Continental Carbon Sink. *Science* **331**: 50.

Bru, D., A., S., and Philippot, L. (2007) Relative abundances of proteobacterial membrane-bound and periplasmic nitrate reductases in selected environments. *Appl Environ Microbiol* **73**: 5971-5974.

Byrne, N., Strous, M., Crepeau, V., Kartal, B., Birrien, J., Schmid, M., *et al*. (2009) Presence and activity of anaerobic ammonium-oxidizing bacteria at deep-sea hydrothermal vents. *ISME J* **3**: 117-123.

Cadillo-Quiroz, H., Bräuer, S., Yashiro, E., Sun, C., Yavitt, J., and Zinder, S. (2006) Vertical profiles of methanogenesis and methanogens in two contrasting acidic peatlands in central New York State, USA. *Environ Microbiol* **8**: 1428-1440.

Cai, C., Hu, S., Chen, X., Ni, B.-J., Pu, J., and Yuan, Z. (2018) Effect of methane partial pressure on the performance of a membrane biofilm reactor coupling methane-dependent denitrification and anammox. *Sci Total Environ* **639**: 278-285.

Dalsgaard, T., and Thamdrup, B. (2002) Factors controlling anaerobic ammonium oxidation with nitrite in marine sediments. *Appl Environ Microbiol* **68**: 3802-3808.

Dalsgaard, T., Thamdrup, B., Farías, L., and Revsbech, N.P. (2012) Anammox and denitrification in the oxygen minimum zone of the eastern South Pacific. *Limnol Oceanogr* **57**: 1331-1346.

Deutzmann, J.S., and Schink, B. (2011) Anaerobic oxidation of methane in sediments of Lake Constance, an oligotrophic freshwater lake. *Appl Environ Microbiol* **77**: 4429-4436.

Deutzmann, J.S., Stief, P., Brandes, J., and Schink, B. (2014) Anaerobic methane oxidation coupled to denitrification is the dominant methane sink in a deep lake. *Proc Natl Acad Sci USA* **111**: 18273-18278.

Ettwig, K.F., van Alen, T., van de Pas-Schoonen, K.T., Jetten, M., and Strous, M. (2009) Enrichment and molecular detection of denitrifying methanotrophic bacteria of the NC10 phylum. *Appl Environ Microbiol* **75**: 3656-3662.

Ettwig, K., Butler, M.K., Le Paslier, D., Pelletier, E., Mangenot, S., Kuypers, M.M., *et al*. (2010) Nitrite-driven anaerobic methane oxidation by oxygenic bacteria. *Nature* **464**: 543-548.

Galloway, J.N., Dentener, F.J., Capone, D.G., Boyer, E.W., Howarth, R.W., Seitzinger, S.P., *et al*. (2004) Nitrogen Cycles: Past, Present, and Future. *Biogeochemistry* **70**: 153-226.

Graf, J.S., Mayr, M.J., Marchant, H.K., Tienken, D., Hach, P.F., Brand, A., *et al*. (2018) Bloom of a denitrifying methanotroph, "*Candidatus* Methylomirabilis limnetica", in a deep stratified lake. *Environ Microbiol* **20**: 2598-2614.

Hamersley, M.R., Woebken, D., Boehrer, B., Schultze, M., Lavik, G., and Kuypers, M.M. (2009) Water column anammox and denitrification in a temperate permanently stratified lake (Lake Rassnitzer, Germany). *Syst Appl Microbiol* **32**: 571-582.

Harhangi, H.R., Le Roy, M., van Alen, T., Hu, B.L., Groen, J., Kartal, B., *et al*. (2012) Hydrazine synthase, a unique phylomarker with which to study the presence and biodiversity of anammox bacteria. *Appl Environ Microbiol* **78**: 752-758.

Haroon, M., Hu, S., Shi, Y., Imelfort, M., Keller, J., Hugenholtz, P., *et al*. (2013) Anaerobic oxidation of methane coupled to nitrate reduction in a novel archaeal lineage. *Nature* **500**: 567-570.

He, Z., Zhang, Q., Feng, Y., Luo, H., Pan, X., and Gadd, G.M. (2018) Microbiological and environmental significance of metal-dependent anaerobic oxidation of methane. *Sci Total Environ* **610-611**: 759-768.

Hou, L., Zheng, Y., Liu, M., Gong, J., Zhang, X., Yin, G., and You, L. (2013) Anaerobic ammonium oxidation (anammox) bacterial diversity, abundance, and activity in marsh sediments of the Yangtze Estuary. *J Geophys Res: Biogeo* **118**: 1237-1246.

Hu, B., Shen, L.D., Lian, X., Zhu, Q., Liu, S., Huang, Q., *et al*. (2014) Evidence for nitrite-dependent anaerobic methane oxidation as a previously overlooked microbial methane sink in wetlands. *Proc Natl Acad Sci USA* **111**: 4495-4500.

Hui, C., Guo, X., Sun, P., Lin, H., Zhang, Q., Liang, Y., and Zhao, Y.H. (2017) Depth-specific distribution and diversity of nitrite-dependent anaerobic ammonium and methane-oxidizing bacteria in upland-cropping soil under different fertilizer treatments. *Appl Soil Ecol* **113**: 117-126.

Jetten, M., Op den Camp, H.J.M., Kuenen, J.G., and Strous, M. (2010) Description of the order Brocadiales. In *In: Krieg NR, Staley JT, Hedlund BP, Paster BJ, Ward N, Ludwig W, Whitman WB (eds) Bergey's manual of systematic bacteriology*. Heidelberg, Germany: Springer, pp. 506-603.

Kampman, C., Piai, L., Temmink, H., Hendrickx, T.L.G., Zeeman, G., and Buisman, C.J.N. (2018) Effect of low concentrations of dissolved oxygen on the activity of denitrifying methanotrophic bacteria. *Water Sci Technol* **77**: 2589-2597.

Kuypers, M.M.M., Lavik, G., Woebken, D., Schmid, M., Fuchs, B.M., Amann, R., *et al*. (2005) Massive nitrogen loss from the Benguela upwelling system through anaerobic ammonium oxidation. *Proc Natl Acad Sci USA* **102**: 6478-6483.

Lam, P., Jensen, M.M., Lavik, G., McGinnis, D.F., Muller, B., Schubert, C.J., *et al*.

(2007) Linking crenarchaeal and bacterial nitrification to anammox in the Black Sea. *Proc Natl Acad Sci USA* **104**: 7104-7109.

Lam, P., Lavik, G., Jensen, M.M., van de Vossenberg, J., Schmid, M., Woebken, D., *et al*. (2009) Revising the nitrogen cycle in the Peruvian oxygen minimum zone. *Proc Natl Acad Sci USA* **106**: 4752-4757.

Lansdown, K., Heppell, C.M., Dossena, M., Ullah, S., Heathwaite, A.L., Binley, A., *et al*. (2014) Fine-scale in situ measurement of riverbed nitrate production and consumption in an armored permeable riverbed. *Environ Sci Technol* **48**: 4425-4434.

Lansdown, K., McKew, B.A., Whitby, C., Heppell, C.M., Dumbrell, A.J., Binley, A. *et al*. (2016) Importance and controls of anaerobic ammonium oxidation influenced by riverbed geology. *Nat Geosci* **9**: 357-360.

Lopez-Gutierrez, J.C., Henry, S., Hallet, S., Martin-Laurent, F., Catroux, G., and Philippot, L. (2004) Quantification of a novel group of nitrate-reducing bacteria in the environment by real-time PCR. *J Microbiol Meth* **57**: 399-407.

Luesken, F., Wu, M.L., Op den Camp, H.J., Keltjens, J.T., Stunnenberg, H., Francoijs, K.J., *et al*. (2012) Effect of oxygen on the anaerobic methanotroph '*Candidatus* Methylomirabilis oxyfera': kinetic and transcriptional analysis. *Environ Microbiol* **14**: 1024-1034.

Meyer, R.L., Risgaard-Petersen, N., and Allen, D.E. (2005) Correlation between anammox activity and microscale distribution of nitrite in a subtropical mangrove sediment. *Appl Environ Microbiol* **71**: 6142-6149.

Mulder, A., van de Graaf, A.A., Robertson, L.A., and Kuenen, J.G. (1995) Anaerobic ammonium oxidation discovered in a denitrifying fluidized bed reactor. *FEMS Microbiol Ecol* **16**: 177-183.

Muyzer, G., de Waal, E., and Uitterlinden, A.G. (1993) Profiling of complex microbial populations by denaturing gradient gel electrophoresis analysis of polymerase chain reaction-amplified genes coding for 16S rRNA. *Appl Environ Microbiol* **59**: 695-700.

Raghoebarsing, A.A., Pol, A., van de Pas-Schoonen, K.T., Smolders, A.J.P., Ettwig, K.F., Rijpstra, W.I.C., *et al*. (2006) A microbial consortium couples anaerobic methane oxidation to denitrification. *Nature* **440**: 918-921.

Rich, J.J., Dale, O.R., Song, B., and Ward, B.B. (2008) Anaerobic ammonium oxidation (anammox) in Chesapeake Bay sediments. *Microb Ecol* **55**: 311-320.

Risgaard-Petersen, N., Meyer, R.L., Schmidt, M., MSM., J., Prast, A., and Rysgaard, S. (2004) Anaerobic ammonia oxidation in an estuarine sediment. *Aquat Microb Ecol* **36**: 293-304.

Rooks, C., Schmid, M.C., Mehsana, W., and Trimmer, M. (2012) The depth-specific significance and relative abundance of anaerobic ammonium-oxidizing bacteria in estuarine sediments (Medway Estuary, UK). *FEMS Microbiol Ecol* **80**: 19-29.

Schubert, C.J., Durisch-Kaiser, E., Wehrli, B., Thamdrup, B., Lam, P., and Kuypers, M.M.M. (2006) Anaerobic ammonium oxidation in a tropical freshwater system (Lake Tanganyika). *Environ Microbiol* **8**: 1857-1863.

Schubert, C.J., Vazquez, F., Losekann-Behrens, T., Knittel, K., Tonolla, M., and Boetius, A. (2011) Evidence for anaerobic oxidation of methane in sediments of a freshwater system (Lago di Cadagno). *FEMS Microbiol Ecol* **76**: 26-38.

Shelley, F., Grey, J., and Trimmer, M. (2014) Widespread methanotrophic primary production in lowland chalk rivers. *Proc Biol Sci* **281**: 20132854.

Shelley, F., Abdullahi, F., Grey, J., and Trimmer, M. (2015) Microbial methane cycling in the bed of a chalk river: oxidation has the potential to match

methanogenesis enhanced by warming. *Freshwat Biol* **60**: 150-160.

Shelley, F., Klaar, M., Krause, S., and Trimmer, M. (2017) Enhanced hyporheic exchange flow around woody debris does not increase nitrate reduction in a sandy streambed. *Biogeochemistry* **136**: 353-372.

Shen, L.D., Liu, S., Huang, Q., Lian, X., He, Z.F., Geng, S., *et al*. (2014) Evidence for the cooccurrence of nitrite-dependent anaerobic ammonium and methane oxidation processes in a flooded paddy field. *Appl Environ Microbiol* **80**: 7611-7619.

Shen, L.D., Hu, B.L., Liu, S., Chai, X.P., He, Z.F., Ren, H.X. *et al*. (2016) Anaerobic methane oxidation coupled to nitrite reduction can be a potential methane sink in coastal environments. *Appl Microbiol Biotechnol* **100**: 7171-7180.

Shen, L.D., Wu, H.S., Liu, X., and Li, J. (2017) Cooccurrence and potential role of nitrite- and nitrate-dependent methanotrophs in freshwater marsh sediments. *Water Res* **123**: 162-172.

Shen, L.D., Ouyang, L., Zhu, Y., and Trimmer, M. (2018) Active pathways of anaerobic methane oxidation across contrasting riverbeds. *ISME J* doi: 10.1038/s41396-018-0302-y.

Stanley, E.H., Casson, N.J., Christel, S.T., Crawford, J.T., Loken, L.C., and Oliver, S.K. (2016) The ecology of methane in streams and rivers: patterns, controls, and global significance. *Ecol Monogr* **86**: 146-171.

ter Braak, C.J.F., and Šmilauer, P. (2005) CANOCO Reference Manual and CanoDraw for Windows User's Guide: Software for Canonical Community Ordination (Version 4.5) Microcomputer Power (Ithaca NY, USA).

Thamdrup, B., and Dalsgaard, T. (2002) Production of N_2 through anaerobic ammonium oxidation coupled to nitrate reduction in marine sediments. *Appl Environ Microbiol* **68**: 1312-1318.

Thamdrup, B., Dalsgaard, T., Jensen, M.M., Ulloa, O., Farías, L., and Escribano, R. (2006) Anaerobic ammonium oxidation in the oxygen-deficient waters off northern Chile. *Limnol Oceanogr* **51**: 2145-2156.

Trimmer, M., Nicholls, J.C., Morley, N., Davies, C.A., and Aldridge, J. (2005) Biphasic behavior of anammox regulated by nitrite and nitrate in an estuarine sediment. *Appl Environ Microbiol* **71**: 1923-1930.

Trimmer, M., and Nicholls, J.C. (2009) Production of nitrogen gas via anammox and denitrification in intact sediment cores along a continental shelf to slope transect in the North Atlantic. *Limnol Oceanogr* **54**: 577-589.

Trimmer, M., Shelley, F.C., Purdy, K.J., Maanoja, S.T., Chronopoulou, P.M., and Grey, J. (2015) Riverbed methanotrophy sustained by high carbon conversion efficiency. *ISME J* **9**: 2304-2314.

Vaksmaa, A., Luke, C., van Alen, T., Vale, G., Lupotto, E., Jetten, M.S., and Ettwig, K.F. (2016) Distribution and activity of the anaerobic methanotrophic community in a nitrogen-fertilized Italian paddy soil. *FEMS Microbiol Ecol* **92**: pii: fiw181.

Wang, J., Cai, C., Li, Y., Hua, M., Wang, J., Yang, H., *et al*. (2018) Denitrifying anaerobic methane oxidation: a previously overlooked methane sink in intertidal zone. *Environ Sci Technol* doi: 10.1021/acs.est.8b05742.

Wang, S., Zhu, G., Peng, Y., Jetten, M.S.M., and Yin, C. (2012) Anammox Bacterial Abundance, Activity, and Contribution in Riparian Sediments of the Pearl River Estuary. *Environ Sci Technol* **46**: 8834-8842.

Wenk, C.B., Blees, J., Zopfi, J., Veronesi, M., Bourbonnais, A., Schubert, C.J., *et al*. (2013) Anaerobic ammonium oxidation (anammox) bacteria and sulfide-dependent denitrifiers coexist in the water column of a meromictic south-alpine lake. *Limnol Oceanogr* **58**: 1-12.

Wu, M.L., Ettwig, K.F., Jetten, M.S.M., Strous, M., Keltjens, J.T., and van Niftrik, L. (2011) A new intra-aerobic metabolism in the nitrite-dependent anaerobic methane-oxidizing bacterium *Candidatus* 'Methylomirabilis oxyfera'. *Biochem Soc Trans* **40**:243-248.

Yan, J., Op den Camp, H.J.M., Jetten, M.S.M., Hu, Y.Y., and Haaijer, S.C.M. (2010) Induced cooperation between marine nitrifiers and anaerobic ammonium-oxidizing bacteria by incremental exposure to oxygen. *Syst Appl Microbiol* **33**: 407-415.

Zhang, M., Luo, Y., Lin, L., Lin, X., Hetharua, B., Zhao, W., *et al*. (2018) Molecular and stable isotopic evidence for the occurrence of nitrite-dependent anaerobic methane-oxidizing bacteria in the mangrove sediment of Zhangjiang Estuary, China. *Appl Microbiol Biotechnol* **102**: 2441-2454.

Zhao, Y., Xia, Y., Kana, T.M., Wu, Y., Li, X., and X., Y. (2013) Seasonal variation and controlling factors of anaerobic ammonium oxidation in freshwater river sediments in the Taihu Lake region of China. *Chemosphere* **93**: 2124-2131.

Zhou, L., Wang, Y., Long, X.-E., Guo, J., and Zhu, G. (2014a) High abundance and diversity of nitrite-dependent anaerobic methane-oxidizing bacteria in a paddy field profile. *FEMS Microbiol Lett* **360**: 33-41.

Zhou, S., Borjigin, S., Riya, S., Terada, A., and Hosomi, M. (2014b) The relationship between anammox and denitrification in the sediment of an inland river. *Sci Total Environ* **490**: 1029-1036.

Zhu, B., van Dijk, G., Fritz, C., Smolders, A.J., Pol, A., Jetten, M.S., and Ettwig, K.F. (2012) Anaerobic oxidization of methane in a minerotrophic peatland: enrichment of nitrite-dependent methane-oxidizing bacteria. *Appl Environ Microbiol* **78**: 8657-8665.

Zhu, G., Wang, S., Wang, W., Wang, Y., Zhou, L., Jiang, B. *et al*. (2013) Hotspots of

anaerobic ammonium oxidation at land–freshwater interfaces. *Nat Geosci* **6**: 103: 357-360.

Zhu, G., Wang, S., Li, Y., Zhuang, L., Zhao, S., Wang, C. *et al*. (2018) Microbial pathways for nitrogen loss in an upland soil. *Environ Microbiol* **20**: 1723-1738.

Figure legends

Figure 1 PCA ordination diagram of pore water chemistries within the different riverbeds (**A**), and differences in potential rates of both anammox (**B**), and n-damo (**C**), across the different riverbeds as a function of that fine-scale chemical variation. Red circles denote the Hammer Stream, blue circles denote the remaining sandy riverbeds, and magenta circles denote the gravel riverbeds. In **A**, PC1 accounted for 51% of the variance and comprised strong negative loadings for O_2 and NO_3^-, and strong positive loading for CH_4. This axis was interpreted as a chemical gradient moving from less reduced to more reduced pore water (Shen *et al*., 2018). PC2 was most strongly associated with NO_2^- (positive); however, this axis explained only 24% of the variance. **B** and **C**, the PC1 score values were obtained from PCA and higher scores are characteristic of more reduced riverbeds, while lower PC1 scores suggest less reduced conditions.

Figure 2 Vertical distributions of both anammox and n-damo in the different riverbeds. **A** and **C** give the potential rates for each process, and **B** and **D** show their respective gene abundances. Both facets of anammox can be described by a common profile (single smoother), where the different riverbeds are treated as random effects on the intercept, the circles denote the different riverbeds and the lines denote the fixed effects from the GAMM. The patterns in n-damo were more complex (**C, D**) requiring three models (intercept and smoother) grouped by red, blue and magenta for the Hammer Stream, the remaining sandy riverbeds and the gravel riverbeds, respectively.

Figure 3 Vertical profiles of the gene abundances of *nap*A (**A**) and *nar*G (**B**) in less permeable sandy riverbeds (red icon) and more permeable gravel riverbeds (blue icon). Note: these copy numbers were natural logarithm–transformed.

Figure 4 RDA ordination plots for the first two principal components of the relationship between pore water chemistries and different microbial processes in the Hammer Stream (red circles), the remaining sandy riverbeds (blue circles) and the gravel riverbeds (magenta circles). PC1 accounted for 57% of the variance and PC2 accounted for 14% of the variance. (R) denotes rate; (A) denotes gene abundance.

Figure 5 Correlations between potential rates of denitrification and anammox in all riverbeds (**A**), and denitrification and n-damo only for the sandy riverbeds (**B**) with a

positive n-damo potential; correlations between *nar*G gene abundance and n-damo bacterial 16S rRNA gene abundance in all riverbeds (**C**), and *nar*G gene abundance and potential n-damo rates only for the sandy riverbeds (**D**). Note: the *r* values for the linear and non-linear models for the correlation between denitrification rates and n-damo rates are 0.657 and 0.851, respectively, and the *r* values for the linear and non-linear models for the correlation between *nar*G gene abundance and n-damo rates are 0.653 and 0.746, respectively.

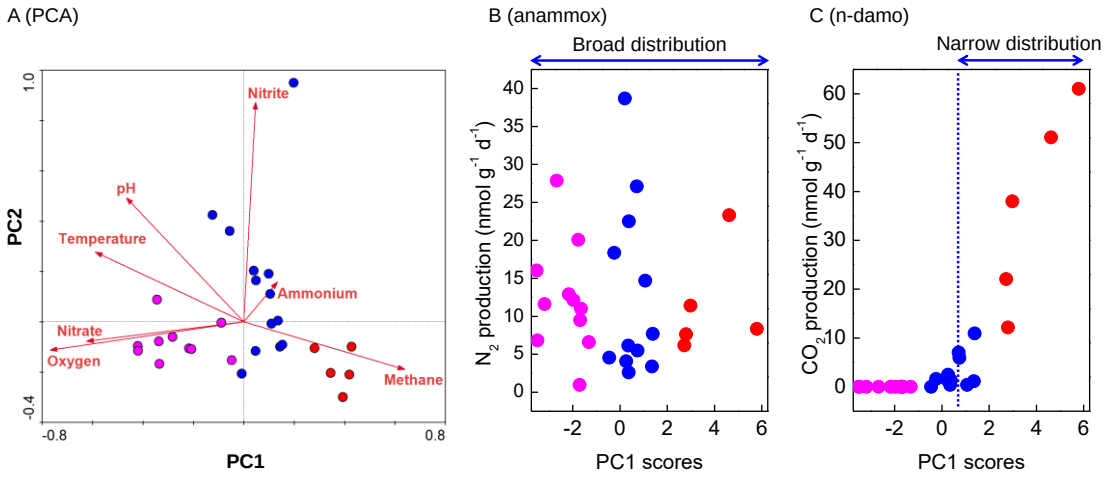

Figure 1

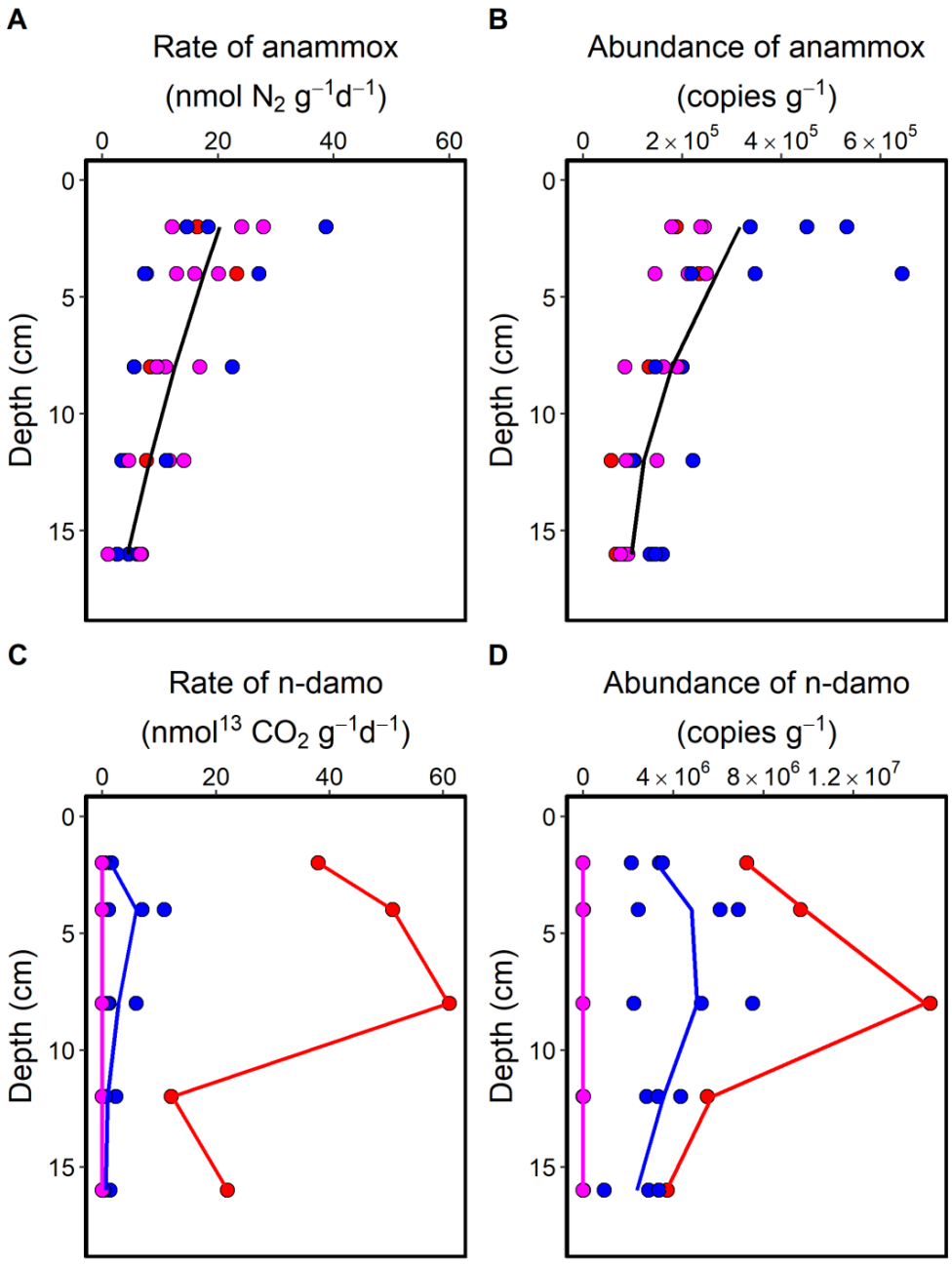

Figure 2

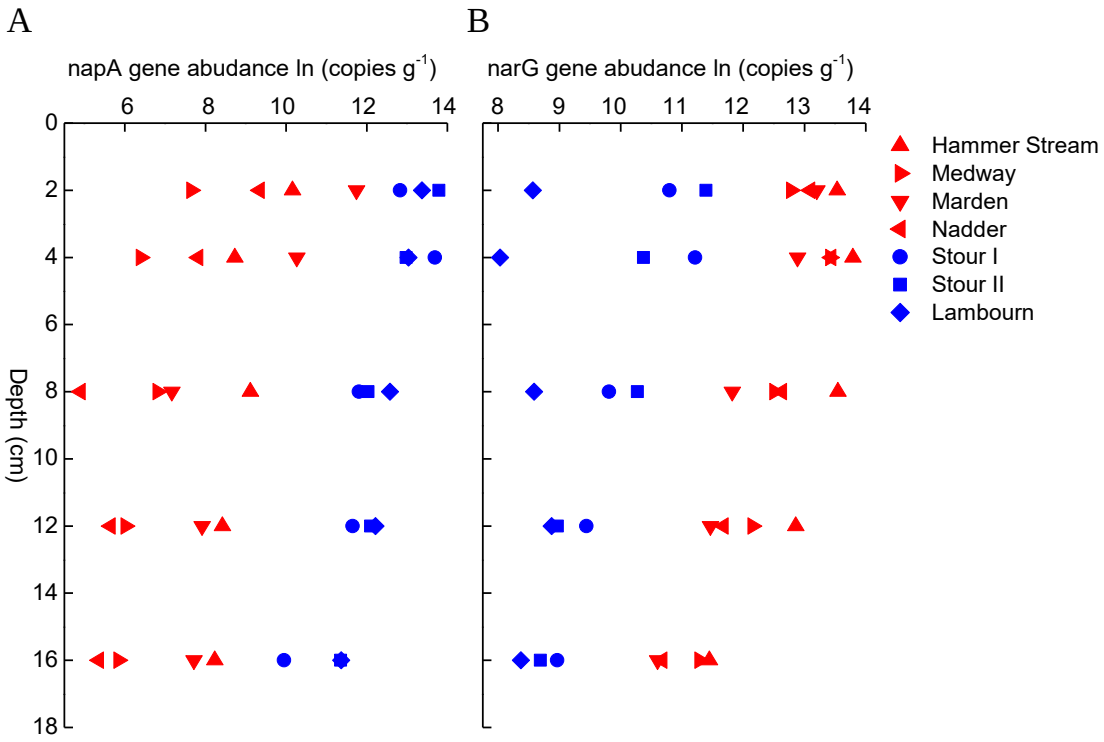

Figure 3

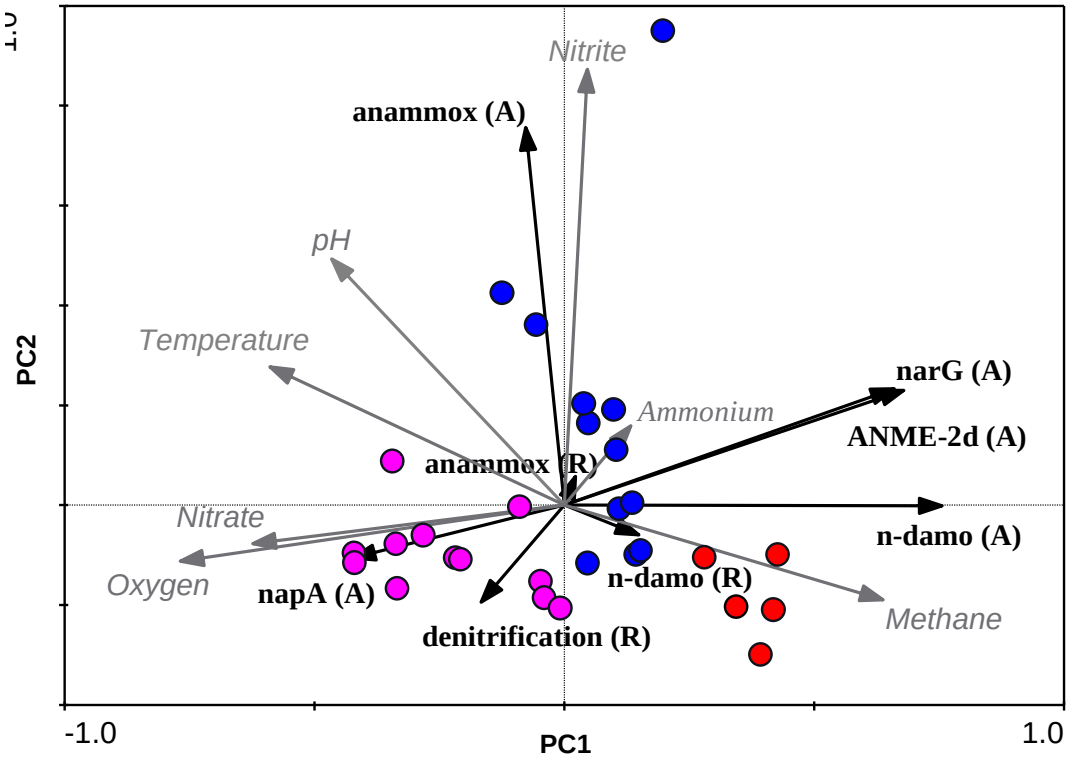

Figure 4

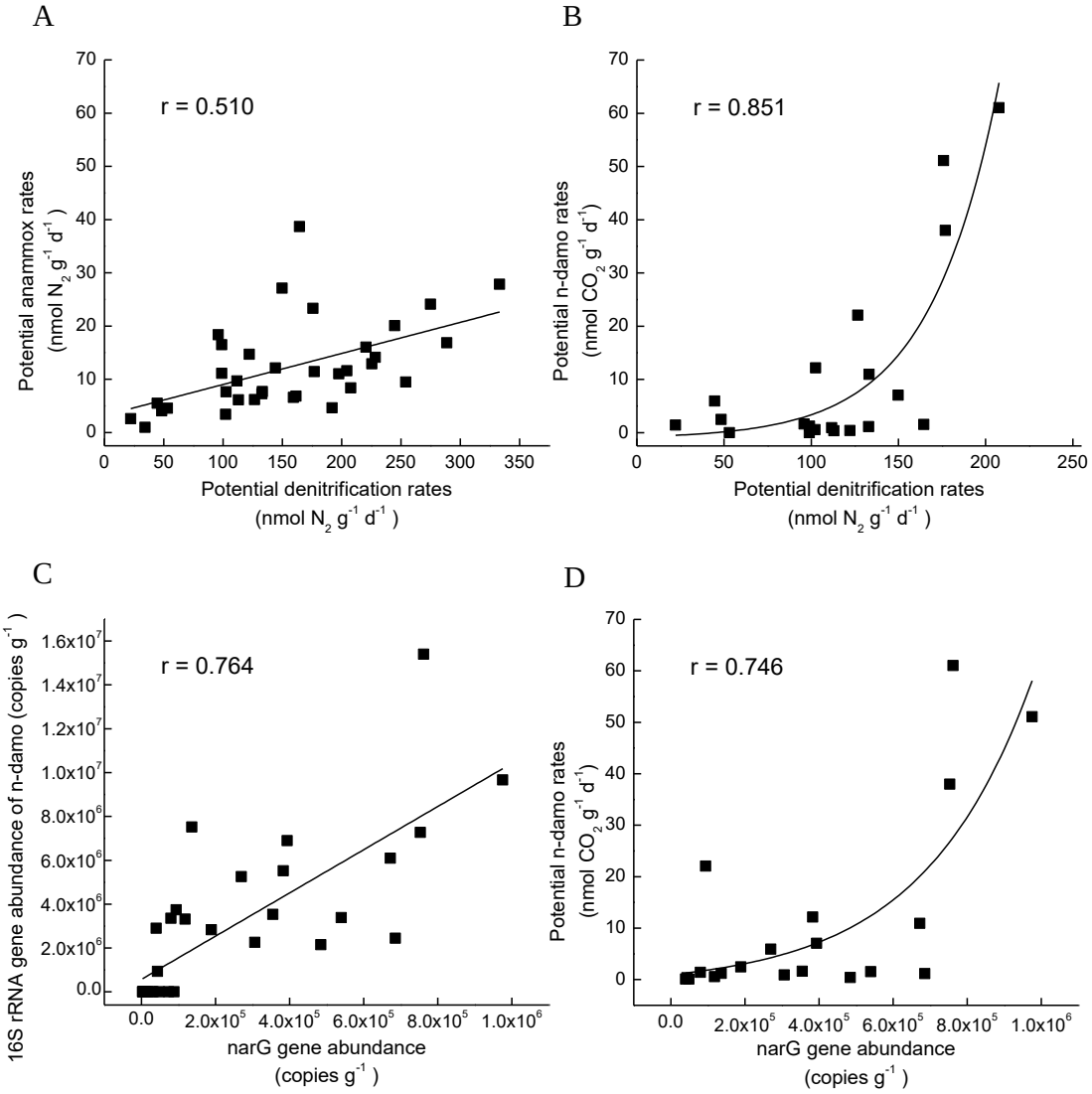

Figure 5